JOURNAL OF CHEMICAL INFORMATION AND MODELING

Article

pubs.acs.org/jcim

Structural Effects of pH and Deacylation on Surfactant Protein C in an Organic Solvent Mixture: A Constant-pH MD Study

Catarina A. Carvalheda,[†] Sara R. R. Campos,[†] Miguel Machuqueiro,[‡] and António M. Baptista*[,†]

[†]Instituto de Tecnologia Química e Biológica, Universidade Nova de Lisboa, Av. da República, EAN, 2780-157 Oeiras, Portugal

[‡]Centro de Química e Bioquímica, Faculdade de Ciências da Universidade de Lisboa, Campo Grande, C8, 1749-016 Lisboa, Portugal

Supporting Information

ABSTRACT: The pulmonary surfactant protein C (SP-C) is a small highly hydrophobic protein that adopts a mainly helical structure while associated with the membrane but misfolds into a β-rich metastable structure upon deacylation, membrane dissociation, and exposure to the neutral pH of the aqueous alveolar subphase, eventually leading to the formation of amyloid aggregates associated with pulmonary alveolar proteinosis. The present constant-pH MD study of the acylated and deacylated isoforms of SP-C in a chloroform/methanol/water mixture, often used to mimic the membrane environment, shows that the loss of the acyl groups has a structural destabilizing effect and that the increase of pH promotes intraprotein contacts which contribute to the loss of helical structure in solution. These contacts result from the poor solvation of charged groups by the solvent mixture, which exhibits a limited membrane-mimetic character. Although a single SP-C molecule was used in the simulations, we propose that analogous intermolecular interactions may play a role in the early stages of the protein misfolding and aggregation in this mixture.

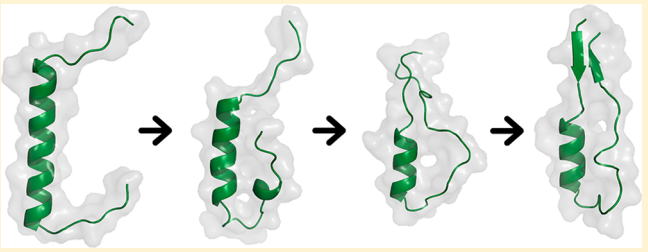

1. INTRODUCTION

The lung surfactant protein C (SP-C) is synthesized in the type II pneumocyte cells of the alveolar wall, being translated into a proprotein that is cleaved and acylated during its transport toward the alveolar surface.[1−3] Once at the alveolar air/water interface, this protein plays a crucial role in preventing the loss of surfactant material during the compression and expansion cycles of the respiratory cycle.[4−7] However, SP-C was found to be involved in pulmonary alveolar proteinosis (PAP), an amyloid disease characterized by the accumulation of surfactant material in the alveolar space.[8,9] Dimeric forms of SP-C were shown to be toxic,[10−12] and the analysis of the bronchoalveolar fluid of PAP patients identified SP-C as the main component of the aggregated material mostly in its deacylated isoform.[13]

The mature SP-C is a small and highly hydrophobic polypeptide chain consisting of a transmembrane helix region and a disordered N-terminal segment.[14−17] The high conservation of SP-C sequence across species clearly indicates a conserved structure: the valine-rich helix region exhibits only a few localized Val/Leu/Ile variations and a strictly conserved lysine−arginine dibasic pair near the helix start, while the N-terminal segment exhibits more variability, though containing a pair of conserved palmitoylated cysteines flanked by prolines.[1,15,17,18] The human form contains 35 amino acid residues, with the transmembrane region comprised between the positions 9 to 34 and exhibiting three basic residues (H9, K11, and R12), while the N-terminal segment contains two palmitoylated cysteines (C5 and C6).

Although the helical structure of this protein has been shown to be the thermodynamically most stable state in a membrane environment, its misfolding to an aggregated β-rich form and concomitant fibril formation have been observed in experimental studies of SP-C in solution.[13,19−22] In this way, the α-helical monomeric state of SP-C seems to be a metastable intermediate in solution, which may undergo $\alpha \rightarrow \beta$ transitions that ultimately result in amyloid fibril formation, depending on the kinetics of particular pathways available and the milieu in which the protein resides.

There are multiple factors that contribute to the SP-C misfolding. The loss of the acyl moieties in a membrane environment was observed to cause a reduction in the protein α-helical content,[23−25] facilitate the protein removal from the membrane,[22,26] and accelerate the rate of fibril formation.[13,20] Once in solution, the valine-rich region has a high β-strand propensity[27] and the exposure to the aqueous alveolar subphase, where the pH is ∼7,[28] is likely to promote the protein misfolding and aggregation into amyloid-like fibrils.[19−22] While the acylated SP-C isoform was shown to form amyloid fibrils under neutral[13,21,29] and acidic[19,20,29] conditions, in a particular study from Dluhy and co-workers,[22] it was observed that with the increase of pH from acidic (1.8) to alkaline (8.2) conditions the deacylated isoform starts to lose its α-helical (native-like) conformation to adopt a β-rich structure that aggregates and ultimately leads to amyloid fibril formation. Furthermore, the pH increase from acidic to alkaline conditions was observed to lead to SP-C deacylation and consequent oligomerization,[30] which is likely to occur via intermolecular disulfide bond formation.

Received: August 12, 2013

   dx.doi.org/10.1021/ci400479c | J. Chem. Inf. Model. XXXX, XXX, XXX−XXX

Since the structural stability of SP-C is especially sensitive to its environment and due to its extremely hydrophobic nature, computer simulation methods are perfect candidates to study the effect of the aforementioned factors on the misfolding process from an atomic point of view. Some work was already done in this respect, namely, the study of the conformational behavior of the deacylated isoform in different pure solvents (chloroform, methanol, or water).[31−34] In particular, Kovacs and co-workers[31,32] have observed that the deacylated SP-C is more stable in water and methanol in comparison to chloroform because the latter was shown to be unable to properly solvate the charged residues of the protein, which ended up forming intramolecular interactions with the polar backbone groups. The authors have also observed a preference of the polar solvents toward the interaction with the polar and polar charged residues of the protein, contrasting with a clear preference of the chloroform molecules toward the apolar protein surface. Nonetheless, short simulation times were always used in the studies done so far, and the dependence of the helix stability on pH and/or deacylation was not addressed.

Here we present a constant-pH molecular dynamics (MD) study of the pH and deacylation effects on the conformational stability of SP-C in a chloroform/methanol/water mixture identical to the one used for its structure determination,[16] with the aim of getting insight into the structural effects that might take part on the early events of the protein misfolding and precede the aggregation process in such medium. We have performed a total of 30 simulations for each isoform considering six different pH values (in the range of 3 to 8), using the stochastic titration constant-pH MD method,[35−38] corresponding to a total of 6 μs. This method can properly model the protonation−conformation coupling in large systems, which makes it suitable to study pH-dependent secondary structure changes, eventually related to misfolding,[39,40] as in the case of SP-C.

Our approach to derive model compound pK_a values from experimental data[35] is here extended to solvent media where no such data are available, using a thermodynamic cycle whose transfer free energies are obtained from Poisson−Boltzmann calculations. Thus, we started by computing model compound pK_a values in water for the GROMOS 54A7 force field and then applied this extension to derive the values in the solvent mixture used here.

Our results show that the stability of both the acylated and deacylated isoforms is affected by pH variation, with the loss of structure starting mostly in the C-terminal region. The loss of the acyl groups is found to result in a lower stability and a higher N-terminal plasticity at acidic and neutral pH conditions. We also observe that the solvent has a reduced ability to stabilize the charged residues, which promotes the formation of contact intraprotein interactions with pH increase, contributing to the loss of helix structure and occasional formation of β motifs. Though not allowed in our single-molecule simulations, we hypothesize that similar stabilizing contact interactions may occur between different SP-C molecules in solution, facilitating the formation of β structure. The solvent mixture is also found to be unable to form extended molecular-level phase separations resembling the amphipathic moieties of a membrane environment, indicating a limited membrane-mimetic character. Overall, this study provides insight into the causes of the pH-dependent helical loss exhibited by SP-C in this medium.

2. METHODS

2.1. Surfactant Protein C Structure. The starting point structure used was the acylated isoform of porcine SP-C (PDB code 1SPF) obtained by 2D NMR methods in a chloroform/methanol/0.1 HCl (32:64:5, v/v/v) mixture.[16] From the 20 available entries in the PDB file, five were chosen to be used as initial structures (replicates) and mutated at five positions using PyMOL[41] to obtain the sequence of the human SP-C (L1F, R2G, N9H, V15I, and V23I) according to ref 18. These correspond to substitutions at some of the few residue positions in SP-C that show variability across different species,[1,15,17,18] with the first two taking place in the disordered N-terminal segment, the third at the very start of the helix, and the last two in the middle of the helix. For the simulations with the acylated isoform, both cysteines were palmitoylated using PyMOL, and the force field parameters for the palmitoyl groups were adapted from the D6PC building block in the GROMOS 45A3 force field[42] (see Table S1 in Supporting Information for further details).

2.2. Solvent Mixture. The conformational behavior of SP-C was studied in a mixture of chloroform/methanol/water (32:64:5 v/v/v or 4:16:3 in terms of molar ratios), resembling the one used for its structure determination.[16] For water, the simple point charge model[43] was used, whereas for methanol and chloroform, the models of GROMOS96 54A7 were chosen. For details on the solvent mixture preparation, consult the Supporting Information.

2.3. System Setup. The different initial structures were placed in rhombic dodecahedral boxes filled with the equilibrated solvent mixture. The boxes had different sizes containing between 1078:4719:924 and 1418:6173:1233 chloroform/methanol/water molecules in the systems with the deacylated isoform and containing between 1237:5479:1078 and 1756:7819:1538 chloroform/methanol/water molecules in the systems with the acylated isoform, always ensuring approximately the same solvent mixture composition used in the structure determination. The systems were energy-minimized and initialized according to the procedure described in the Supporting Information.

2.4. Constant-pH MD Simulations. Each of the five initialized systems was then simulated at six different pH values (3, 4, 5, 6, 7, and 8) during 100 ns using the in-house constant-pH MD algorithm: the stochastic titration method.[35−38] This method consists of a cycle with three main steps: (1) a Poisson−Boltzmann/Monte Carlo (PB/MC) step that computes the protonation free energies for a specific protein conformation at a given pH and assigns the new protonation states according to the last MC move; (2) an MD segment, here taken as 0.2 ps long, where the solute molecule is kept rigid, allowing for the adaptation of the solvent molecules to the new solute charge configuration; (3) an MD segment, here taken as 2 ps long, of the whole unconstrained system, which samples the conformational space for the selected protonation state, and whose last sampled conformation is used for a new PB/MC calculation in the following cycle. The MD and PB/MC settings are described in the following sections.

We note that the inclusion of pH 8 in our set of simulations is mainly intended to better cover the pH range used in ref 22, but as mentioned above, previous experimental studies of SP-C in a similar chloroform/methanol mixture have shown that extensive deacylation and oligomerization start to occur between pH 7 and pH 8 (persisting at higher pH), presumably associated

dx.doi.org/10.1021/ci400479c | J. Chem. Inf. Model. XXXX, XXX, XXX−XXX

with the formation of interprotein disulfide bonds.[30] Therefore, our simulations at pH 8 are generally inadequate for both the acylated and deacylated isoforms and should be regarded as representing only the small subpopulations of molecules unaffected by deacylation and/or oligomerization. Their comparison with experimental data should thus be done with reservations.

2.5. MD Settings. All the MD simulations were performed with the GROMACS package version 3.2.1,[44,45] using the GROMOS96 54A7 force field[46] and applying periodic boundary conditions. The nonbonded interactions were treated with the neighbor searching approach using a twin-range method with a lower cutoff of 0.8 nm and an upper cutoff of 1.4 nm beyond which the van der Waals interactions were neglected. The neighbor list was updated each five simulation steps (10 fs), and the Coulombic interactions were treated with the reaction field approach[47] in the minimization/initialization phases, while the generalized reaction field approach[48] was used in the MD steps of the constant-pH MD runs. The dielectric constant of the mixture was calculated using Oster's rule[49] and set to 24.7, while the isothermal compressibility was calculated assuming that the volume of the mixture was approximately the sum of the volumes of the original components and set to 1.272×10^{-4} bar^{-1}, and the ionic strength was set to 150 mM. The temperature was set to 310 K and the pressure to 1 atm using the Berendsen thermostat and barostat algorithms,[50] with respective time constants of 0.1 and 2 ps and separate coupling for the protein and the solvent mixture.

2.6. PB/MC Settings. The electrostatic energies for each protonated state were calculated using the MEAD package (version 2.2.8).[51] The atomic charges and radii were taken from the GROMOS 54A7 force field as described elsewhere,[52] and the molecular surface was defined with a solvent probe of radius 1.4 Å and a Stern layer of 2.0 Å. The temperature was set to 310 K, the ionic strength was 150 mM, and the dielectric constants were 2 in the molecular interior and 24.7 in the solvent mixture (calculated using Oster's rule[49]). A two-step focusing procedure[53] was employed using a grid spacing of 1.0 and 0.25 Å. The pK_a values of the model compounds in the solvent mixture were determined as described below. The protonation states were sampled by MC simulations using the program PETIT (version 1.5)[54] and performing 10^5 MC steps for each calculation. Each step consisted of a cycle of random choices of state (including tautomeric forms) for all individual sites and for pairs of sites with coupling above 2.0 pK_a units,[54,55] whose acceptance/rejection followed a Metropolis criterion.[56]

We have considered five titratable sites in the deacylated isoform (the N-terminal amine, C5 and C6 thiol, H9 imidazole, and the C-terminal carboxyl) and three titratable residues in the acylated isoforms (N-terminal, H9 and C-terminal), with the K11 side chain amino and the R12 guanidinium always being protonated.

2.7. Model Compound pK_a Values in the Solvent Mixture. The pK_a values of the model compounds required for the PB/MC calculations were obtained along the lines of ref 38, whose proposed methodology can be briefly described as follows: (1) each model compound is taken as a suitable molecular fragment whose pK_a value is initially undetermined; (2) a simple reference molecule is selected which contains such fragment as the only protonatable site and for which the pK_a value is known; (3) constant-pH MD simulations are run for this reference molecule using an arbitrary pK_a model, which is corrected afterward by simply shifting the resulting titration curve to match the experimental one. This procedure makes the model compound pK_a an unambiguous and well-defined quantity, but the computed values are force-field-specific and rely on the existence of experimental pK_a values for the reference molecules in the solvent of interest. We have previously determined model compound pK_a values in water for the GROMOS force fields 43A1 and 53A6, using as reference molecules the set of pentapeptides experimentally studied by Pace and co-workers,[57] but no similar titration data seem to exist for the particular solvent mixture used in the present study. Therefore, we introduced a variation on the previous methodology that can be generally adopted when no such data are available.

We started by determining the model pK_a values in water for the GROMOS 54A7 force field following the same methodology as in ref 38, namely, using the same definition of molecular fragments, the same tautomeric fractions, and the same experimental data.[57] The model compound pK_a values thus obtained for water, pK_{mod}^{wat}, are shown in Table 1. By considering

Table 1. Model Compound pK_a Values in Water Using the GROMOS96 54A7 Force Field

residue	pK_{mod}^{wat}
Asp	3.73
Glu	4.19
His	6.88
Cys	8.58
Tyr	9.59
Lys	10.48
Arg	13.65
Cter	3.19
Nter	7.96

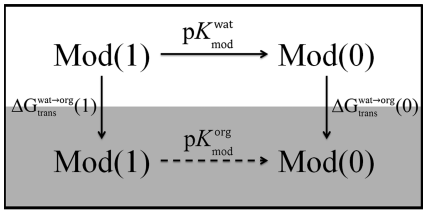

Figure 1. Thermodynamic cycle used for the computation of the protonation free energies of the model compounds in the chloroform/methanol/water mixture, pK_{mod}^{org}.

the thermodynamic cycle depicted in Figure 1, the pK_a values of the model compounds of interest in the chloroform/methanol/water mixture, pK_{mod}^{org}, were computed from the pK_{mod}^{wat} values and the transfer free energies of each model compound from water to the solvent mixture, $\Delta G_{trans}^{wat \rightarrow org}$, in both its protonated (1) and deprotonated (0) forms. Since preliminary MD simulations showed a homogeneous solvent mixture without actual phase separations (as observed in the protein simulations; see section 3), a simple PB model was used to compute the transfer free energies, using MEAD[51] as described above. The resulting pK_{mod}^{org} values are presented in section 3.

2.8. Analyses. All the analyses were performed using GROMACS software or in-house tools. Only the last 75 ns of each trajectory was used in the analyses, being considered the equilibrated segment in all simulations after inspection of several properties. The protein secondary structure was assigned using the DSSP criterion defined by Kabsch and Sander.[58]

dx.doi.org/10.1021/ci400479c | J. Chem. Inf. Model. XXXX, XXX, XXX−XXX

The root-mean-square fluctuation (rmsf) for each amino acid residue was determined after C^{α} least-squares fit of all the structures to the helical region of a central structure.[59] All errors were computed using standard correlation-correcting algorithms,[60] and the within- and across-replicates errors were combined using the law of total variance.[61] The titration curves were obtained by averaging at each pH value the occupancy states of the titratable sites over the final equilibrated segment.[37] The data were fitted to the Hill equation, $f(\mathrm{pH}) = [1 + 10^{n(\mathrm{pH}-\mathrm{p}K_a)}]^{-1}$, where n represents the Hill coefficient, using the nonlinear least-squares Marquardt–Levenberg algorithm[62] implemented in gnuplot 4.0,[63] and the corresponding asymptotic standard errors were used as uncertainties of the fitted parameters. All the presented molecular representations were done using PyMOL.[41]

3. RESULTS AND DISCUSSION

3.1. Helix Stability: pH and Acylation Effects. To understand the effect of pH and acylation on SP-C stability, the secondary structure of both the deacylated and acylated isoforms was analyzed in the studied pH range. Inspection of the temporal evolution of the secondary structure in all simulations (Figures S1–S6 in Supporting Information) shows that the replicate-averaged helix content is stabilized after the equilibration period (first 25 ns), while the occurrence of β structure was a very rare and transient event.

As mentioned in the Introduction, experimental works reported that the removal of the acyl moieties in a membrane environment corresponds to a decrease in the helix content.[23−25] In agreement with these results, we observe a decrease at neutral and acidic pH conditions in our simulations (Figure 2), with

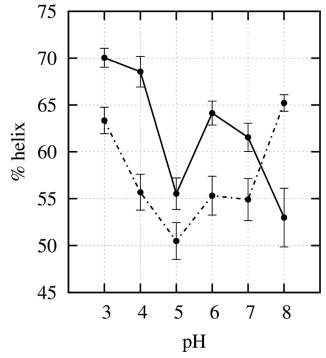

Figure 2. Percentage of helix content as a function of pH for both the acylated (filled line) and deacylated (dashed line) isoforms of SP-C. The percentage of helix content accounts for the contribution of the α-helix, 3-helix, and 5-helix motifs.

the acyl groups stabilizing the N-terminal region of the protein (Figure 3, left). At pH 8, the acylation seems to have the opposite effect, being associated with a greater loss of helical content, which is due to a significant loss of structure in a single replicate (green line in Figure S6, without which the average helical content is 58 ± 2%). In any case, as indicated in section 2.4, the simulations at pH 8 are intended to reflect only a small subpopulation of SP-C molecules that resist deacylation and cannot be directly related to experimental data.

Considering the acylated isoform, the extreme acidic conditions do not seem to destabilize the helix conformation since a native-like helical content was obtained at pH 3 and 4. This seems to be consistent with the structural NMR study of

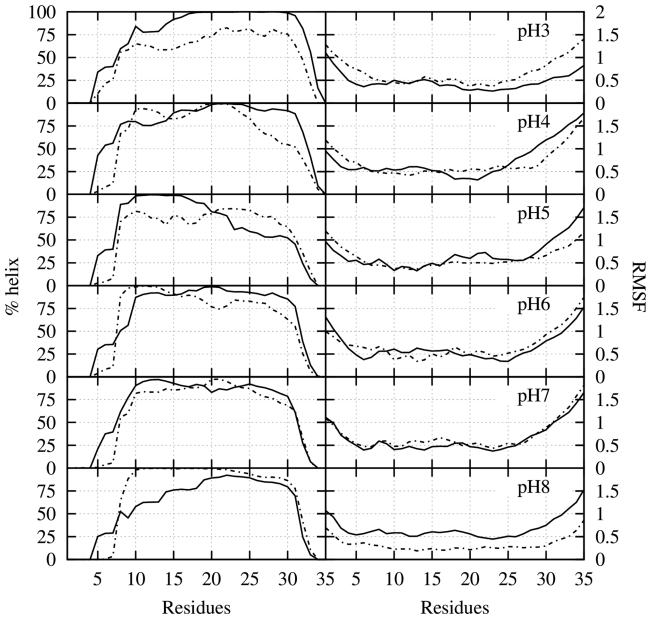

Figure 3. Percentage of time that each residue spends in the helix conformation (left) and rmsf for each residue (right) for both the acylated (filled line) and deacylated (dashed line) isoforms of SP-C, at different pH values.

the acylated isoform of porcine SP-C,[16] which was done using a $CHCl_3/CH_3OH$/0.1 M HCl 32:64:5 (v/v/v) mixture whose pH value, although not reported in the article, should be at most a few units above the 1.0 value of the initial aqueous solution, considering the value 1.8 measured in a similar $CHCl_3/CH_3OH$/0.1 M HCl 10:70:4 (v/v/v) mixture,[22] as well as the general trend observed in other organic solvent mixtures.[64,65] Thus, the acylated porcine SP-C structure obtained by NMR should correspond to a low pH value, in agreement with the stable structure observed here in that pH region for its human counterpart in the same solvent; such interspecies agreement is not surprising, considering that the sequence of the hydrophobic helix is highly conserved (two Val/Ile substitutions) and that the remaining three substitutions (see section 2.1) are located in the disordered N-terminal segment. Some helical loss is observed at pH 6 and 7 and a more marked one at pH 5 and 8. Nevertheless, these results cannot be directly compared with the experimental studies of the acylated isoform[13,19−21] since the experimental results for different pH conditions were obtained using different techniques or variations of the same technique that can affect the conformational behavior of the protein. In addition, as addressed in section 2.4, the simulations at pH 8 should not be directly related to the experimental full-population data.

Dluhy and co-workers[22] observed that the continuing increase of the pH from acidic conditions (∼1.8) to alkaline conditions (∼8.2) in a similar solvent mixture promotes $\alpha \rightarrow \beta$ transitions and protein aggregation events of the deacylated isoform, which result in the formation of amyloid motifs. In agreement with these experimental results, we observe a decrease in the helix content of deacylated SP-C from pH 3 to 5 followed by a slight increase at pH 6 and 7 (more pronounced in our study). At pH 8, the conservation of the helix content at the same levels as pH 6 and 7 is not reproduced by our simulations, but, as already pointed out, those simulations are expected to represent only the small subpopulation of

dx.doi.org/10.1021/ci400479c | J. Chem. Inf. Model. XXXX, XXX, XXX−XXX

monomeric SP-C present at this pH.[30] As already noted above, the formation of β structure was not statistically significant, being very rare and transient (Figures S1−S6 in Supporting Information).

Despite the lack of experimental evidence about where the loss of structure begins and where the β motifs start to form, some computational studies for the deacylated isoform have already revealed some interesting results on this matter.[32−34] The unfolding of the deacylated protein was observed to start in the C-terminal region in water, chloroform, or methanol,[32,33] but in the presence of other deacylated SP-C molecules and considering a water environment, the loss of structure was shown to start in the N-terminal region.[34] In our simulations, the occasional formation of β structure arises from the interactions between the N- and C-terminal unfolded regions in the majority of the cases, as illustrated in Figure 4A, with the loss

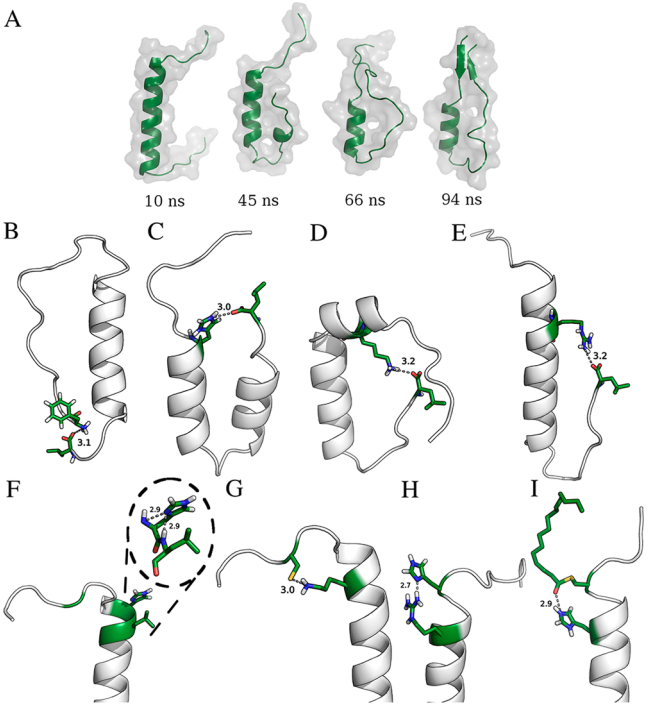

Figure 4. Cartoon representations of the formation of β structure in one of the deacylated SP-C replicates simulated at pH 5 (A) and the most common intraprotein contact interactions: of the carboxyl group of the C-terminal residue with the amine group of the N-terminal residue (B), with the imidazole group of H9 (C), with the amino group of K11 (D), and with the guanidinium group of R12 (E); of the imidazole $N^{\delta 1}$ atom of H9 with the backbone nitrogen atom of both H9 and L10 (F); of the thiol group of the deacylated C5 with the amino group of K11 (G); of the imidazole group of H9 with the guanidinium group of R12 (H) and with the acyl oxygen of the of the acylated C5 (I). The distances are in Å.

of structure being more prone to start at the C-terminal region (~55 and ~70% of the cases in the acylated and deacylated isoforms, respectively). We observe that in some cases the protein is able to recover some helical structure and that a decrease in helical content seldom implies the formation of β structure (Figures S1−S6 in the Supporting Information).

As expected, the root-mean-square fluctuations of the protein residues (Figure 3, right) show a greater flexibility in the termini regions, especially in the C-terminal, which together with a greater tendency to lose helical structure suggests a greater plasticity of these regions (in the C-terminal, particularly). These results also show that the deacylation increases the flexibility of the N-terminal under acidic conditions.

3.2. Intraprotein Contact Interactions and Ionization.

Inspection of the protein conformation along the simulations shows that the loss of helical structure is often associated with intraprotein interactions, as the between termini ones mentioned above. Such interactions result in frequent contacts between particular pairs of residues, depicted in Figure 4B−I, which involve one or two ionizable residues. Given that the charge state of those ionizable residues depends on pH, this results in a pH-dependent coupling between conformation and protonation.

The mean protonation of each titratable site at each pH value was used to compute its titration curve (Figure 5) and its pK_a

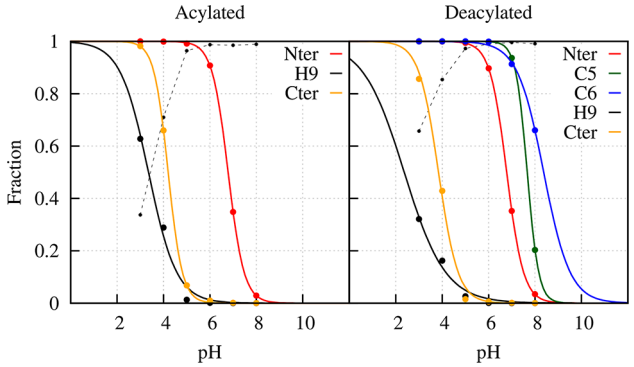

Figure 5. Titration curves of the sites considered titratable in the constant-pH MD simulations of both the acylated (left) and deacylated (right) isoforms of SP-C (filled line) and fraction of the H9 $N^{\epsilon 2}$-H tautomer, where only the imidazole $N^{\epsilon 2}$ atom has a proton (dashed line). The Nter and Cter sites correspond to, respectively, the N-terminal amine and the C-terminal carboxyl groups. The points are the average protonations obtained from the simulations, and the lines are the corresponding fits to Hill curves (see section 2.8). For the errors of the average protonations, see Figures S15 and S16 in Supporting Information.

Table 2. Computed pK_a Values and Respective Asymptotic Standard Errors for the Sites Considered Titratable in the Constant-pH MD Runs of Both the Deacylated and Acylated Isoforms and Respective pK_{mod} Values

	pK_a		
residue	acylated	deacylated	pK_{mod}
Nter	6.78 ± 0.11	6.78 ± 0.13	6.98
C5		7.66 ± 0.07	9.85
C6		8.37 ± 0.22	9.85
H9	3.35 ± 0.14	2.37 ± 0.25	5.91
Cter	4.20 ± 0.27	3.84 ± 0.32	3.52

values (Table 2) (Hill coefficients and additional protonation data given in Supporting Information). Although not experimentally available, the "typical" pK_a value of each titrable site in the solvent mixture (e.g., when inserted in a short alanine peptide[57]) is expected to differ only slightly from the corresponding pK_{mod} value in Table 2, as for the case in aqueous solution (see ref 38 and Table 1).

We observe a very high negative shift from the pK_{mod} for the H9 site in both isoforms with a strong stabilization of its neutral state and from the pK_{mod} for the C5 site in the deacylated form with a strong stabilization of its charged state, both indicating

dx.doi.org/10.1021/ci400479c | J. Chem. Inf. Model. XXXX, XXX, XXX−XXX

strong intraprotein interactions. In spite of the other sites exhibiting smaller negative or positive shifts from their pK_{mod} values, the different values obtained for the acylated and deacylated forms also point to structural effects. To further understand each interaction, the relation between the frequency of contacts and the protonation states of the involved residues was analyzed (Figures 6 and 7).

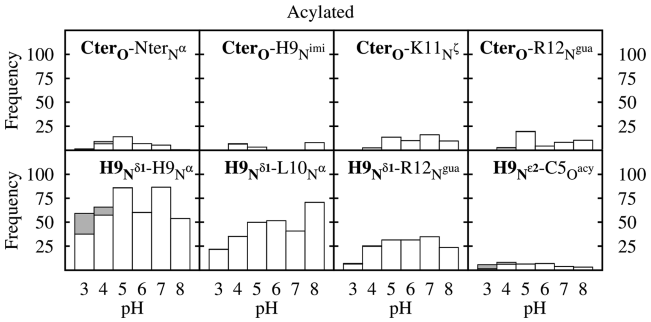

Figure 6. Frequency of occurrence of several contact interactions in acylated SP-C at different pH values, with the empty/filled bar regions indicating the deprotonated/protonated fraction of the titratable residue shown in bold (when in contact). Atom designations: O refers to any of the two C-terminal carboxyl oxygens, N^{imi} to either $N^{\delta1}$ or $N^{\varepsilon2}$, N^{gua} to any of the guanidinium nitrogen atoms, and O^{acy} to the carbonyl oxygen of the acyl moiety. Contacts were considered to occur when the shortest distance between the two indicated set of atoms was lower than either 6 Å (top plots) or 4 Å (bottom plots), these thresholds corresponding approximately to the minima of the population histogram in each case.

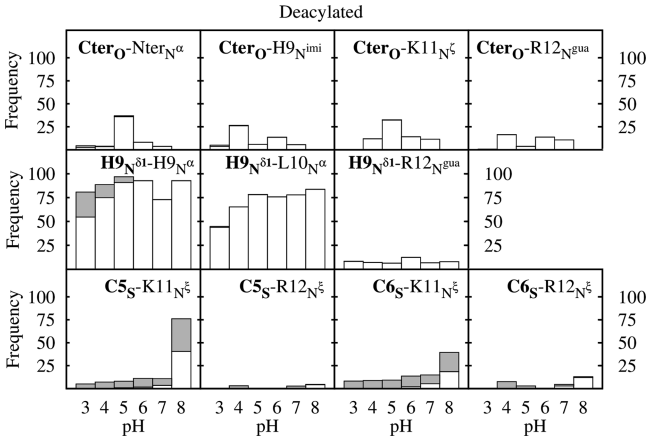

Figure 7. Frequency of occurrence of several contact interactions in deacylated SP-C at different pH values, with the empty/filled bar regions indicating the deprotonated/protonated fraction of the titratable residue shown in bold (when in contact). Atom designations: O refers to any of the two C-terminal carboxyl oxygens, N^{imi} to either $N^{\delta1}$ or $N^{\varepsilon2}$, N^{gua} to any of the guanidinium nitrogen atoms, and S to the sulfur atom in the thiol group. Contacts were considered to occur when the shortest distance between the two indicated set of atoms was lower than either 6 Å (top plots) or 4 Å (middle and bottom plots), these thresholds corresponding approximately to the minima of the population histogram in each case.

Starting with the H9 residue, the most frequent contacts are maintained between the imidazole $N^{\delta1}$ atom and the backbone N atoms of both H9 and L10, especially in the deacylated isoform (Figure 4F, Figure 6, bottom, and Figure 7, middle). These simultaneous contacts conformationally trap H9 and strongly favor its deprotonated state where only the imidazole $N^{\varepsilon2}$ atom has a proton ($N^{\varepsilon2}$-H tautomer, Figure 5, dashed line). In the acylated isoform, this behavior is not so pronounced at low pH (Figure 5, dashed line, and Figure 6, bottom) because the contacts with the R12 guanidinium nitrogen atoms (Figure 4H) happen in both tautomeric states, and the additional contact between the H9 $N^{\varepsilon2}$ atom and the carbonyl group of the acyl moieties (Figure 4I) can happen in the protonated state, rescuing H9 from its trapped configuration in the $N^{\varepsilon2}$-H tautomer. Thus, contacts between the $N^{\delta1}$ atom and the backbone nitrogen atoms of both the H9 and L10 residues explain the large shift in the H9 titration curve for both SP-C isoforms, while the lesser number of these contacts and the interactions between H9 and both R12 and the acyl moieties (mainly the C5 one) are likely to explain the less pronounced shift of the acylated isoform.

Several contacts were observed involving the carboxyl group of the C-terminal residue (Cter) and the positively charged residues (Nter, H9, K11, and R12), hereafter referred to as end-to-end interactions (Figure 4B–E). The occurrence of these interactions is associated with the loss of helical structure, eventually leading to the formation of β motifs, as they bring the terminal regions close together (Figure 4A). The contacts are mainly established between the deprotonated C-terminal residue and K11 and R12 (Figure 6 and Figure 7, top) and are more abundant in deacylated SP-C up to pH 6, thus stabilizing the ionized state of the C-terminal carboxyl group and explaining why its pK_a is lower for this isoform. At pH 7 and 8, the end-to-end interactions are much reduced in the deacylated case because cysteine sites (C5 and C6) start to ionize and compete with the C-terminal site for the contacts with both K11 and R12 (Figure 7, bottom). These competing contacts become dominant at pH 8, especially with the C5 site, thereby stabilizing its ionized state and resulting in a pK_a lower than that of C6.

Overall, the intraprotein contact interactions are closely associated with the structural changes observed in the simulations. In particular, the end-to-end interactions seem to lead to partial helix disruption, with the loss of helical content being clearly correlated with the formation of such contacts (Figure 8, top). When we consider all the intraprotein contacts (Figure 8, bottom), the trend for the acylated isoform is mostly

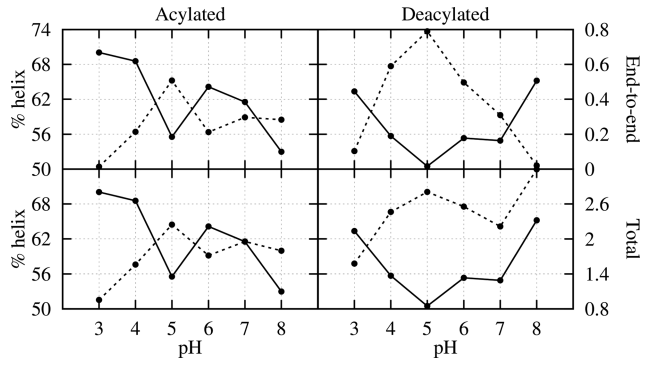

Figure 8. Relation between the percentage of helix (filled line) and the average number of end-to-end (top) and total (bottom) contacts (dashed line) per frame for each pH value for both the acylated (left) and deacylated (right) SP-C isoforms. End-to-end contacts account for the contact interactions of the C-terminal residue with the N-terminal residue, H9, K11, and R12, while total contacts account for all the contact interactions as described in the captions of Figures 6 and 7. The standard errors for the percentage of helix structure are shown in Figure 2, and the standard errors of the average number of end-to-end and total contacts were always lower than 0.07 and 0.14, respectively.

dx.doi.org/10.1021/ci400479c | J. Chem. Inf. Model. XXXX, XXX, XXX–XXX

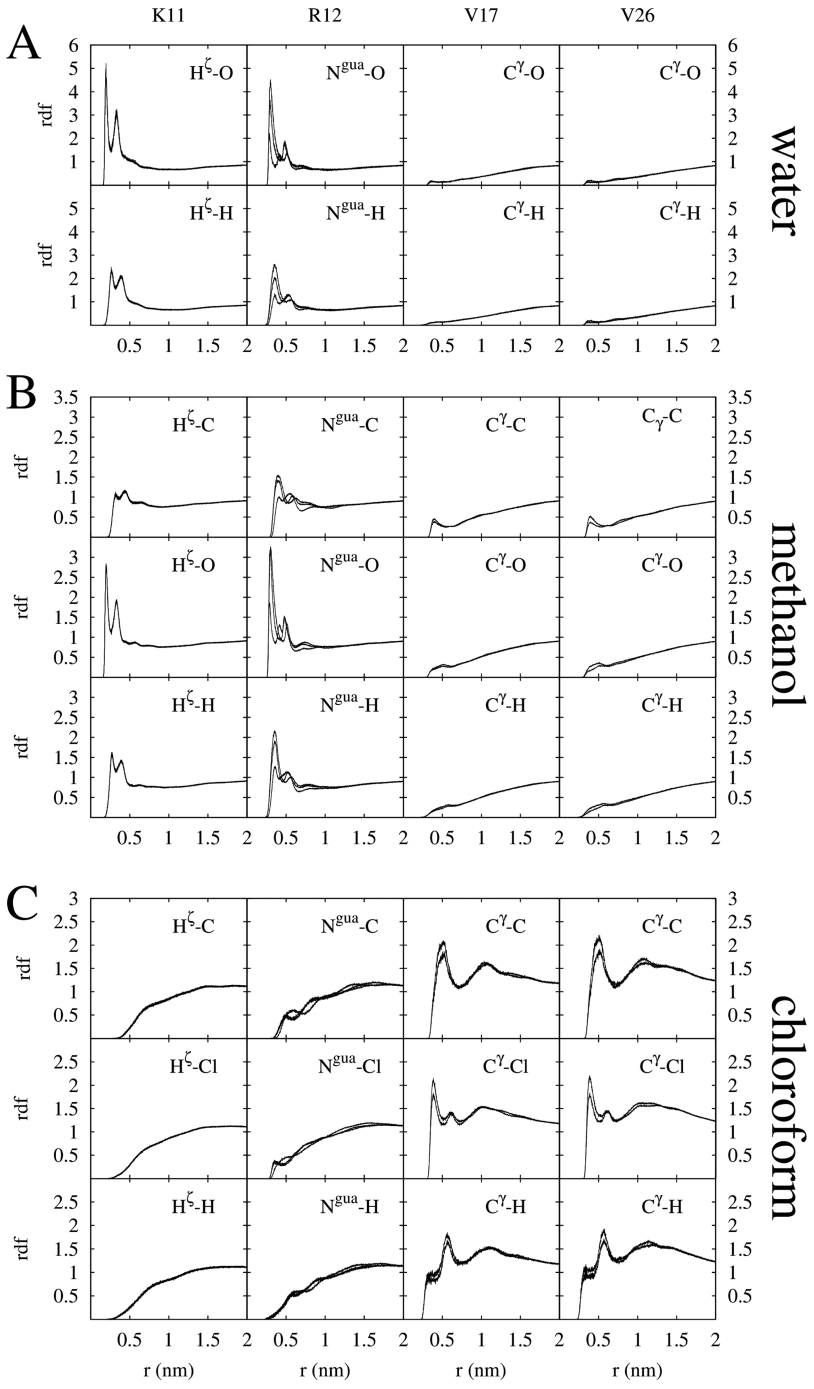

Figure 9. Radial distribution function between SP-C and water (A), methanol (B), and chloroform (C), computed from the simulations of deacylated SP-C at pH 7. From left to right, the SP-C atoms are the three H^{ζ} atoms of K11, the three guanidinium nitrogens of R12 and the two $C^{\gamma 1}$ and $C^{\gamma 2}$ atoms of V17 and V26, each atom represented by an individual curve. The solvent atoms are the oxygen (A, top) and hydrogen (A, bottom) atoms of water, the carbon (B, top), oxygen (B, middle), and hydrogen (B, bottom) atoms of methanol, and the carbon (C, top), chloride (C, middle), and hydrogen (C, bottom) atoms of chloroform; the curves for the water hydrogens and the chloroform chlorides represent an average over the equivalent atoms.

maintained, while the deacylated isoform no longer displays the decrease of contacts at high pH, essentially reflecting the interaction of negative cysteines with the lysine and arginine positive residues also located on the N-terminal portion of the protein. As already noted, the ionization of the cysteine residues and the associated intramolecular interactions observed in our simulations should be regarded with reservations.

As pointed out above, many of the observed intraprotein contact interactions involve oppositely charged groups, indicating a mutual charge stabilization effect that would not be expected in an aqueous environment. This reflects a poor charge solvation ability of the solvent mixture being used, as discussed below.

3.3. Solvent Mixture and Interprotein Interactions. Due to their preferential solvation effects, chloroform/methanol/water mixtures have been extensively used to mimic the membrane environment, including in several experimental studies of the surfactant protein C misfolding.[13,19,20,22] Although the mixture components are completely miscible at the

dx.doi.org/10.1021/ci400479c | J. Chem. Inf. Model. XXXX, XXX, XXX−XXX

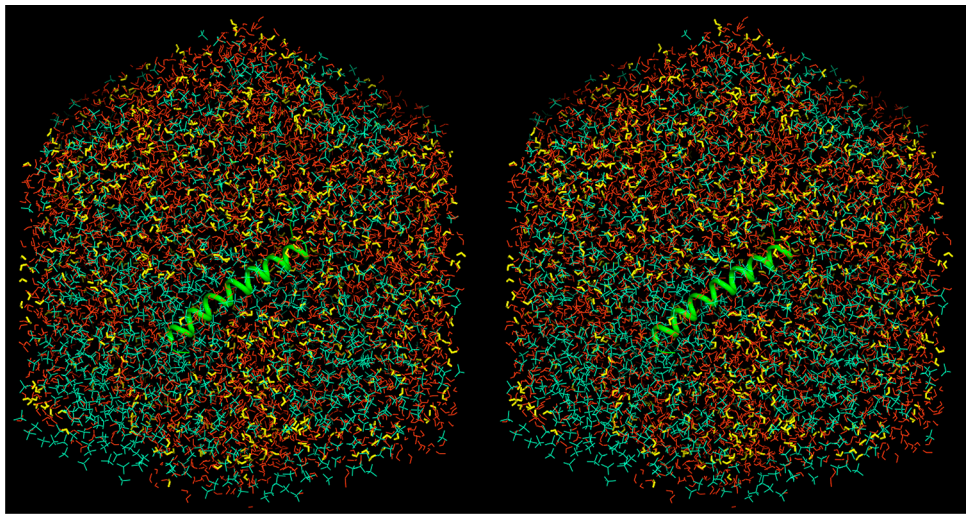

Figure 10. Snapshot of the final configuration of the simulation of deacylated SP-C at pH 3, showing the distribution of the different solvent components chloroform (cyan), methanol (reddish), and water (yellow) around SP-C (light green). Similar distributions were observed during all simulations.

macroscopic level, MD studies show that the chloroform molecules have a preferential solvation for apolar regions and the methanol molecules for polar regions of the solute, which may cause a separation of phases at the microscopic level that is facilitated by the presence of water molecules in solution.[66,67] To investigate if this behavior was also present in our simulations, we computed the radial distribution function of the different solvent molecules in relation to specific polar charged (K11 and R12) and apolar (V17 and V26) residues of the protein. Only the results at pH 7 in the deacylated isoform are shown (Figure 9) and discussed below since the results are essentially identical for the other pH conditions and for the acylated isoform.

For the polar charged residues, we observe a strong interaction with water and methanol and no significant interactions with chloroform. In the interactions between these residues and the water and methanol molecules, a solvent orientation with the negatively charged oxygen atom toward the amino acid positively charged groups is preferred. In contrast, for the apolar residues, a strong preference toward the interaction with chloroform is observed, namely, between the amino acid side chain methyl groups and the chloride atoms of chloroform. These results are in agreement with previous MD studies with chloroform/methanol mixtures[66,67] and with the study done by Kovacs and co-workers in pure solvents.[32]

Despite the distinct preferential solvation of the apolar and charged/polar groups, no extended phase separations were ever observed in our simulations, but only very small and short-ranged transient clusters of either chloroform or methanol molecules (Figure 10). This means that the solvent was unable to form any extensive hydrophilic or hydrophobic layers near the corresponding protein regions, as would be expected to properly mimic a membrane environment. According to a simulation study by Mottamal and co-workers,[67] this ability depends on the ratio of hydrophilic and hydrophobic components, with chloroform-rich and water-containing mixtures yielding more membrane-like solvation properties. These authors have observed an extended, membrane-mimicking phase separation only in a mixture with chloroform/methanol/water molar ratios of 4:4:1 (or 16:16:4 v/v/v), which is substantially richer in chloroform than the mixture used here and in the NMR study,[16] with molar ratios of 4:16:3. This may explain why, despite the observed preferential solvations and small transient clusters, we do not see any extended phase separations (Figure 1 of ref 67 shows the clear difference between both situations; our Figure 10 is a clear example of no phase separation). The amount of chloroform is even lower in the mixture used in the experimental study of the pH-induced structural changes,[22] with molar ratios of 1:15:2, suggesting that such extended phase separations may be even more unlikely in that case.

These considerations indicate that the solvent mixture used in the present study (and in the NMR study) is unable to form the extended hydrophobic/hydrophilic phase separation required to properly mimic a membrane bilayer, meaning that all protein regions tend to experience the overall effect of an essentially homogeneous solvent with a moderate dielectric constant, here estimated to be 24.7 (see section 2.5). Consequently, this mixture has a smaller ability to efficiently solvate the charged/polar groups located in the terminal regions of the protein than their typical physiological environment, where they would be either in the aqueous phase (whose dielectric constant is around 80) or at the lipid−water interface (whose dielectric constant may be even higher[68,69]). In the mixture, such groups get instead stabilized through intraprotein contacts that may require a previous loss of structure (the end-to-end interactions) or not (those involving cysteine or histidine residues) and that were observed to become more frequent with the increase of pH for both isoforms in our simulations (Figure 8, bottom); the fact that such contacts and associated helical loss are largely absent at low pH in the acylated isoform is consistent with the determination of a stable structure in the NMR study, as discussed in section 3.1. The occurrence of intramolecular interactions involving charged groups was also observed by Kovacs and co-workers[31] for deacylated SP-C in pure chloroform, although less extensively than in our simulations, perhaps due to the fact that pure apolar solvents tend to severely restrict protein flexibility.[70]

As discussed above, a similar absence of phase separations probably holds for the chloroform-poor mixture used in the experimental study of the pH-induced misfolding,[22] meaning that charge-stabilizing intramolecular contacts and consequent helix loss may also occur in that case. The same concern may be

extended to other studies of SP-C misfolding using similar mixtures with low chloroform content.[13,19−21]

Although the pH variation does not affect the solvent mixture ability to properly solvate and stabilize charges, it affects the protonation/deprotonation equilibrium of the titratable residues, thereby influencing the intraprotein contacts established and, consequently, the protein conformational behavior. Among the different pH-mediated intraprotein interactions that occur due to the low dielectric constant of the media, the end-to-end interactions are the ones which most affect SP-C conformational behavior at pH 4 to 7, destabilizing its helical conformation and sometimes promoting the formation of β motifs. The less frequent end-to-end interactions in the acylated isoform might explain the greater stability of this isoform at the intermediate simulated pH conditions.

If we consider a picture where several SP-C molecules are present in a chloroform-poor solution, the formation of interprotein interactions will provide a way to stabilize the charged/polar groups, analogously to the stabilizing intraprotein interactions observed in our single-protein simulations. Therefore, we would expect such interprotein interactions to become more frequent with the increase of pH (as in Figure 8, bottom) and to eventually promote $\alpha \rightarrow \beta$ transitions (as in Figure 4A), in agreement with the experimental results at neutral and high pH conditions for the deacylated isoform in such a chloroform-poor mixture.[22] This provides a molecular picture of the effect of pH on the early stages of SP-C misfolding and suggests an important role of the interprotein interactions in promoting the $\alpha \rightarrow \beta$ transitions that precede the formation of the fibrillar aggregates in mixtures that have been used to study this biological process. Nonetheless, the stabilizing role of protein−protein interactions is not expected to be as relevant in a membrane environment, where charged/polar residues can be either properly solvated by the water molecules or interact with the charged/zwitterionic phospholipid headgroups. Though the chloroform/methanol/water mixtures exhibit properties that are suited to solubilize and study amphiphilic (membranar) molecules like SP-C, their use in conformational studies should be considered with caution, especially because they may be unable to provide a true phase separation required for a membrane-like environment.

4. CONCLUDING REMARKS

In this work, we present a constant-pH MD study on the structural effects of deacylation and pH on SP-C in a membrane-mimetic chloroform/methanol/water mixture in order to understand the structural effects that might be involved in the early stages of the protein misfolding. We started by obtaining model compound pK_a values in this mixture by first computing their values in water for the GROMOS 54A7 force field as previously described,[38] and then considering a thermodynamic cycle whose transfer free energies from water to the mixture are calculated using a PB model. Constant-pH MD simulations at several pH values were then performed for both acylated and deacylated SP-C isoforms, each accounting for a total of 3 μs of simulation time.

We have shown that both the pH variations[22] and deacylation[13,20,22−25] affect the conformational behavior of surfactant protein C in a chloroform/methanol/water mixture, in agreement with experimental observations. The loss of helical structure is related to the formation of pH-mediated intraprotein interactions (favored by the media low dielectric constant), which is facilitated by the loss of the acyl chains. These interactions may explain the deacylated SP-C misfolding observed experimentally, with the increase of the pH from acidic (pH 3) to basic (pH 8) conditions resulting in more frequent residue−residue interactions. The formation of β-sheet motifs observed in our simulations usually involves interactions between the N- and C-terminal regions, with the latter being the one where the loss of helix content is more prone to start. Although such residue−residue interactions seem to be insufficient to result in extensive β-sheet formation in our single-protein simulations, when several SP-C molecules are present, they may lead to the aggregation and amyloid fibril formation reported in like-solvent experimental studies.[13,19−22,29] Nonetheless, the inference of the behavior of multiple SP-C molecules from single-molecule simulations is obviously limited.

The methanol and chloroform molecules are found to preferentially interact with, respectively, polar and apolar residues, as previously observed in other simulations of chloroform/methanol mixtures,[66,67] but the absence of a substantial phase separation may explain the need for the charged groups to get stabilized through mutual interactions, a situation unlikely to occur in the native membranar environment. This also suggests that some of the solvent mixtures able to solubilize amphiphilic molecules like SP-C, often used as membrane "substitutes" in experimental studies, may lack the ability to form the molecular-level extended phase separations which would more accurately mimic a membrane environment.

Overall, the present work points to the need to study the SP-C conformational behavior at different pH conditions in a native environment, either via experimental or computer simulation techniques, and the relevance of performing simulations with multiple SP-C molecules either in an organic solvent mixture or in a membrane system. Work along these lines is being conducted.

■ ASSOCIATED CONTENT

Supporting Information

Table with the force field parameters used for the palmitoylated cysteine residues, details on the minimization/initialization procedure, figures with the percentage of helix and β structure for all replicates at each pH value, table with the Hill coefficients for each titratable residue, and figures with the cumulative protonation averages and individual Hill curves for each titratable residue. This material is available free of charge via the Internet at http://pubs.acs.org.

■ AUTHOR INFORMATION

Corresponding Author

*E-mail: baptista@itqb.unl.pt.

Notes

The authors declare no competing financial interest.

■ ACKNOWLEDGMENTS

This study was supported by Fundação para a Ciência e Tecnologia, Portugal, through Grant Nos. PTDC/QUI-BIQ/105238/2008, PEst-OE/EQB/LA0004/2011, and PEst-OE/QUI/UI0612/2013.

■ ABBREVIATIONS

SP-C, surfactant protein C; PAP, pulmonary alveolar proteinosis; MD, molecular dynamics; PDB, Protein Data Bank; D6PC, dihexanoyl phosphatidylcholine; PB, Poisson−Boltzmann; MC, Monte Carlo; rmsf, root-mean-square fluctuations

REFERENCES

(1) Haagsman, H. P.; Diemel, R. V. Surfactant-Associated Proteins: Functions and Structural Variation. *Comp. Biochem. Physiol., Part A: Mol. Integr. Physiol.* **2001**, *129*, 91−108.

(2) Ten Brinke, A.; van Golde, L. M. G.; Batenburg, J. J. Palmitoylation and Processing of the Lipopeptide Surfactant Protein C. *Biochim. Biophys. Acta* **2002**, *1583*, 253−265.

(3) Weaver, T. E. Synthesis, Processing and Secretion of Surfactant Proteins B and C. *Biochim. Biophys. Acta, Mol. Basis Dis.* **1998**, *1408*, 173−179.

(4) Taneva, S.; Keough, K. M. Pulmonary Surfactant Proteins SP-B and SP-C in Spread Monolayers at the Air−Water Interface: II. Monolayers of Pulmonary Surfactant Protein SP-C and Phospholipids. *Biophys. J.* **1994**, *66*, 1149−1157.

(5) Kramer, A.; Wintergalen, A.; Sieber, M.; Galla, H. J.; Amrein, M.; Guckenberger, R. Distribution of the Surfactant-Associated Protein C within a Lung Surfactant Model Film Investigated by Near-Field Optical Microscopy. *Biophys. J.* **2000**, *78*, 458−465.

(6) Takamoto, D. Y.; Lipp, M. M.; von Nahmen, A.; Lee, K. Y.; Waring, A. J.; Zasadzinski, J. A. Interaction of Lung Surfactant Proteins with Anionic Phospholipids. *Biophys. J.* **2001**, *81*, 153−169.

(7) Zuo, Y. Y.; Keating, E.; Zhao, L.; Tadayyon, S. M.; Veldhuizen, R. A. W.; Petersen, N. O.; Possmayer, F. Atomic Force Microscopy Studies of Functional and Dysfunctional Pulmonary Surfactant Films. I. Micro- and Nanostructures of Functional Pulmonary Surfactant Films and the Effect of SP-A. *Biophys. J.* **2008**, *94*, 3549−3564.

(8) Presneill, J. J.; Nakata, K.; Inoue, Y.; Seymour, J. F. Pulmonary Alveolar Proteinosis. *Clin. Chest Med.* **2004**, *25*, 593−613.

(9) Seymour, J. F.; Presneill, J. J. Pulmonary Alveolar Proteinosis: Progress in the First 44 Years. *Am. J. Respir. Crit. Care Med.* **2002**, *166*, 215−235.

(10) Baatz, J. E.; Smyth, K. L.; Whitsett, J. A.; Baxter, C.; Absolom, D. R. Structure and Functions of a Dimeric Form of Surfactant Protein SP-C: A Fourier Transform Infrared and Surfactometry Study. *Chem. Phys. Lipids* **1992**, *63*, 91−104.

(11) Creuwels, L. A.; Demel, R. A.; van Golde, L. M.; Haagsman, H. P. Characterization of a Dimeric Canine Form of Surfactant Protein C (SP-C). *Biochim. Biophys. Acta* **1995**, *1254*, 326−332.

(12) Shen, H. Q.; Duan, C. X.; Li, Z. Y.; Suzuki, Y. Effects of Proteinosis Surfactant Proteins on the Viability of Rat Alveolar Macrophages. *Am. J. Respir. Crit. Care Med.* **1997**, *156*, 1679−1687.

(13) Gustafsson, M.; Thyberg, J.; Näslund, J.; Eliasson, E.; Johansson, J. Amyloid Fibril Formation by Pulmonary Surfactant Protein C. *FEBS Lett.* **1999**, *464*, 138−142.

(14) Curstedt, T.; Johansson, J.; Persson, P.; Eklund, A.; Robertson, B.; Löwenadler, B.; Jörnvall, H. Hydrophobic Surfactant-Associated Polypeptides: SP-C Is a Lipopeptide with Two Palmitoylated Cysteine Residues, Whereas SP-B Lacks Covalently Linked Fatty Acyl Groups. *Proc. Natl. Acad. Sci. U.S.A.* **1990**, *87*, 2985−2989.

(15) Johansson, J.; Persson, P.; Löwenadler, B.; Robertson, B.; Jörnvall, H.; Curstedt, T. Canine Hydrophobic Surfactant Polypeptide SP-C. A Lipopeptide with One Thioester-Linked Palmitoyl Group. *FEBS Lett.* **1991**, *281*, 119−122.

(16) Johansson, J.; Szyperski, T.; Curstedt, T.; Wüthrich, K. The NMR Structure of the Pulmonary Surfactant-Associated Polypeptide SP-C in an Apolar Solvent Contains a Valyl-Rich α-Helix. *Biochemistry* **1994**, *33*, 6015−6023.

(17) Johansson, J. Structure and Properties of Surfactant Protein C. *Biochim. Biophys. Acta* **1998**, *1408*, 161−172.

(18) Johansson, J.; Jörnvall, H.; Eklund, A.; Christensen, N.; Robertson, B.; Curstedt, T. Hydrophobic 3.7 kDa Surfactant Polypeptide: Structural Characterization of the Human and Bovine Forms. *FEBS Lett.* **1988**, *232*, 61−64.

(19) Szyperski, T.; Vandenbussche, G.; Curstedt, T.; Ruysschaert, J. M.; Wüthrich, K.; Johansson, J. Pulmonary Surfactant-Associated Polypeptide C in a Mixed Organic Solvent Transforms from a Monomeric α-Helical State into Insoluble β-Sheet Aggregates. *Protein Sci.* **1998**, *7*, 2533−2540.

(20) Gustafsson, M.; Griffiths, W. J.; Furusjö, E.; Johansson, J. The Palmitoyl Groups of Lung Surfactant Protein C Reduce Unfolding into a Fibrillogenic Intermediate. *J. Mol. Biol.* **2001**, *310*, 937−950.

(21) Hosia, W.; Johansson, J.; Griffiths, W. J. Hydrogen/Deuterium Exchange and Aggregation of a Polyvaline and a Polyleucine α-Helix Investigated by Matrix-Assisted Laser Desorption Ionization Mass Spectrometry. *Mol. Cell. Proteomics* **2002**, *1*, 592−597.

(22) Dluhy, R. A.; Shanmukh, S.; Leapard, J. B.; Krüger, P.; Baatz, J. E. Deacylated Pulmonary Surfactant Protein SP-C Transforms from α-Helical to Amyloid Fibril Structure via a pH-Dependent Mechanism: An Infrared Structural Investigation. *Biophys. J.* **2003**, *85*, 2417−2429.

(23) Johansson, J.; Nilsson, G.; Strömberg, R.; Robertson, B.; Jörnvall, H.; Curstedt, T. Secondary Structure and Biophysical Activity of Synthetic Analogues of the Pulmonary Surfactant Polypeptide SP-C. *Biochem. J.* **1995**, *307*, 535−541.

(24) Wang, Z.; Gurel, O.; Baatz, J. E.; Notter, R. H. Acylation of Pulmonary Surfactant Protein-C Is Required for Its Optimal Surface Active Interactions with Phospholipids. *J. Biol. Chem.* **1996**, *271*, 19104−19109.

(25) Yousefi-Salakdeh, E.; Johansson, J.; Strömberg, R. A Method for S- and O-Palmitoylation of Peptides: Synthesis of Pulmonary Surfactant Protein-C Models. *Biochem. J.* **1999**, *343*, 557−562.

(26) Bi, X.; Flach, C. R.; Pérez-Gil, J.; Plasencia, I.; Andreu, D.; Oliveira, E.; Mendelsohn, R. Secondary Structure and Lipid Interactions of the N-Terminal Segment of Pulmonary Surfactant SP-C in Langmuir Films: IR Reflection−Absorption Spectroscopy and Surface Pressure Studies. *Biochemistry* **2002**, *41*, 8385−8395.

(27) Kallberg, Y.; Gustafsson, M.; Persson, B.; Thyberg, J.; Johansson, J. Prediction of Amyloid Fibril-Forming Proteins. *J. Biol. Chem.* **2001**, *276*, 12945−12950.

(28) Nielson, D. W.; Goerke, J.; Clements, J. A. Alveolar Subphase pH in the Lungs of Anesthetized Rabbits. *Proc. Natl. Acad. Sci. U.S.A.* **1981**, *78*, 7119−7123.

(29) Li, J.; Hosia, W.; Hamvas, A.; Thyberg, J.; Jörnvall, H.; Weaver, T. E.; Johansson, J. The N-Terminal Propeptide of Lung Surfactant Protein C Is Necessary for Biosynthesis and Prevents Unfolding of a Metastable α-Helix. *J. Mol. Biol.* **2004**, *338*, 857−862.

(30) Plasencia, I.; Cruz, A.; López-Lacomba, J. L.; Casals, C.; Pérez-Gil, J. Selective Labeling of Pulmonary Surfactant Protein SP-C in Organic Solution. *Anal. Biochem.* **2001**, *296*, 49−56.

(31) Kovacs, H.; Mark, A. E.; Johansson, J.; van Gunsteren, W. F. The Effect of Environment on the Stability of an Integral Membrane Helix: Molecular Dynamics Simulations of Surfactant Protein C in Chloroform, Methanol and Water. *J. Mol. Biol.* **1995**, *247*, 808−822.

(32) Kovacs, H.; Mark, A. E.; van Gunsteren, W. F. Solvent Structure at a Hydrophobic Protein Surface. *Proteins: Struct., Funct., Bioinf.* **1997**, *27*, 395−404.

(33) Zangi, R.; Kovacs, H.; van Gunsteren, W. F.; Johansson, J.; Mark, A. E. Free Energy Barrier Estimation of Unfolding the α-Helical Surfactant-Associated Polypeptide C. *Proteins: Struct., Funct., Bioinf.* **2001**, *43*, 395−402.

(34) Ramírez, E.; Santana, A.; Cruz, A.; Plasencia, I.; López, G. E. Molecular Dynamics of Surfactant Protein C: From Single Molecule to Heptameric Aggregates. *Biophys. J.* **2006**, *90*, 2698−2705.

(35) Baptista, A. M.; Teixeira, V. H.; Soares, C. M. Constant-pH Molecular Dynamics Using Stochastic Titration. *J. Chem. Phys.* **2002**, *117*, 4184−4200.

(36) Machuqueiro, M.; Baptista, A. M. Constant-pH Molecular Dynamics with Ionic Strength Effects: Protonation−Conformation Coupling in Decalysine. *J. Phys. Chem. B* **2006**, *110*, 2927−2933.

(37) Machuqueiro, M.; Baptista, A. M. Acidic Range Titration of HEWL Using a Constant-pH Molecular Dynamics Method. *Proteins: Struct., Funct., Bioinf.* **2008**, *72*, 289−298.

(38) Machuqueiro, M.; Baptista, A. M. Is the Prediction of pK_a Values by Constant-pH Molecular Dynamics Being Hindered by Inherited Problems? *Proteins: Struct., Funct., Bioinf.* **2011**, *79*, 3437−3447.

(39) Campos, S. R. R.; Machuqueiro, M.; Baptista, A. M. Constant-pH Molecular Dynamics Simulations Reveal a β-Rich Form of the Human Prion Protein. *J. Phys. Chem. B* **2010**, *114*, 12692−12700.
(40) Vila-Viçosa, D.; Campos, S. R. R.; Baptista, A. M.; Machuqueiro, M. Reversibility of Prion Misfolding: Insights from Constant-pH Molecular Dynamics Simulations. *J. Phys. Chem. B* **2012**, *116*, 8812−8821.
(41) DeLano, W. L. The PyMOL Molecular Graphics System; www.pymol.org. Acessed September 19, 2012.
(42) Schuler, L. D.; Daura, X.; van Gunsteren, W. F. An Improved GROMOS96 Force Field for Aliphatic Hydrocarbons in the Condensed Phase. *J. Comput. Chem.* **2001**, *22*, 1205−1218.
(43) Hermans, J.; Berendsen, H. J. C.; van Gunsteren, W. F.; Postma, J. P. M. A Consistent Empirical Potential for Water−Protein Interactions. *Biopolymers* **1984**, *23*, 1513−1518.
(44) Berendsen, H. J. C.; van der Spoel, D.; van Drunen, R. GROMACS: A Message-Passing Parallel Molecular Dynamics Implementation. *Comput. Phys. Commun.* **1995**, *91*, 43−56.
(45) Lindahl, E.; Hess, B.; van der Spoel, D. GROMACS 3.0: A Package for Molecular Simulation and Trajectory Analysis. *J. Mol. Model.* **2001**, *7*, 306−317.
(46) Schmid, N.; Eichenberger, A. P.; Choutko, A.; Riniker, S.; Winger, M.; Mark, A. E.; van Gunsteren, W. F. Definition and Testing of the GROMOS Force-Field Versions 54A7 and 54B7. *Eur. Biophys. J* **2011**, *40*, 843−856.
(47) Barker, J. A.; Watts, R. O. Monte Carlo Studies of the Dielectric Properties of Water-like Models. *Mol. Phys.* **1973**, *26*, 789−792.
(48) Tironi, I. G.; Sperb, R.; Smith, P. E.; van Gunsteren, W. F. A Generalized Reaction Field Method for Molecular Dynamics Simulations. *J. Chem. Phys.* **1995**, *102*, 5451.
(49) Wang, P.; Anderko, A. Computation of Dielectric Constants of Solvent Mixtures and Electrolyte Solutions. *Fluid Phase Equilib.* **2001**, *186*, 103−122.
(50) Berendsen, H. J. C.; Postma, J. P. M.; van Gunsteren, W. F.; DiNola, A.; Haak, J. R. Molecular Dynamics with Coupling to an External Bath. *J. Chem. Phys.* **1984**, *81*, 3684−3690.
(51) Bashford, D.; Gerwert, K. Electrostatic Calculations of the pK_a Values of Ionizable Groups in Bacteriorhodopsin. *J. Mol. Biol.* **1992**, *224*, 473−486.
(52) Teixeira, V. H.; Cunha, C. A.; Machuqueiro, M.; Oliveira, A. S. F.; Victor, B. L.; Soares, C. M.; Baptista, A. M. On the Use of Different Dielectric Constants for Computing Individual and Pairwise Terms in Poisson−Boltzmann Studies of Protein Ionization Equilibrium. *J. Phys. Chem. B* **2005**, *109*, 14691−14706.
(53) Baker, N. A.; Bashford, D.; Case, D. A. In *Implicit Solvent Electrostatics in Biomolecular Simulation*; Springer: Berlin, 2006; Vol. *49*, Chapter V, pp 263−295.
(54) Baptista, A.; Soares, C. Some Theoretical and Computational Aspects of the Inclusion of Proton Isomerism in the Protonation Equilibrium of Proteins. *J. Phys. Chem. B* **2001**, *105*, 293−309.
(55) Baptista, A. M.; Martel, P. J.; Soares, C. M. Simulation of Electron−Proton Coupling with a Monte Carlo Method: Application to Cytochrome c_3 Using Continuum Electrostatics. *Biophys. J.* **1999**, *76*, 2978−2998.
(56) Metropolis, N.; Rosenbluth, A.; Rosenbluth, M.; Teller, A.; Teller, E. Equation of State Calculations by Fast Computing Machines. *J. Chem. Phys.* **1953**, *21*, 1087−1092.
(57) Grimsley, G. R.; Scholtz, J. M.; Pace, C. N. A Summary of the Measured p*K* Values of the Ionizable Groups in Folded Proteins. *Protein Sci.* **2009**, *18*, 247−251.
(58) Kabsch, W.; Sander, C. Dictionary of Protein Secondary Structure: Pattern Recognition of Hydrogen-Bonded and Geometrical Features. *Biopolymers* **1983**, *22*, 2577−2637.
(59) Campos, S. R. R.; Baptista, A. M. Conformational Analysis in a Multidimensional Energy Landscape: Study of an Arginylglutamate Repeat. *J. Phys. Chem. B* **2009**, *113*, 15989−16001.
(60) Allen, M. P.; Tildesley, D. J. In *Computer Simulation of Liquids*; Clarendon Press: Oxford, 1987.
(61) Bertsekas, D. P.; Tsitsiklis, J. N. In *Introduction to Probability*; Athena Scientific: Belmont, MA, 2002.
(62) Press, W. H.; Teukolsky, S. A.; Vetterling, W. T.; Flannery, B. P. In *Numerical Recipes in C++: The Art of Scientific Computing*, 2nd ed.; Cambridge University Press: Cambridge, UK, 2002.
(63) *Gnuplot*; http://www.gnuplot.info/. Acessed February 20, 2013.
(64) Mussini, T.; Covington, A. K.; Longhi, P.; Rondinini, S. Criteria for Standardization of pH Measurements in Organic Solvents and Water + Organic Solvent Mixtures of Moderate to High Permittivities. *Pure Appl. Chem.* **1985**, *57*, 865−876.
(65) Mussini, P. R.; Mussini, T.; Rondinini, S. Reference Value Standards and Primary Standards for pH Measurements in D_2O and Aqueous Organic Solvent Mixtures: New Accessions and Assessments (Technical Report). *Pure Appl. Chem.* **1997**, *69*, 1007−1014.
(66) Gratias, R.; Kessler, H. Molecular Dynamics Study on Microheterogeneity and Preferential Solvation in Methanol/Chloroform Mixtures. *J. Phys. Chem. B* **1998**, *102*, 2027−2031.
(67) Mottamal, M.; Shen, S.; Guembe, C.; Krilov, G. Solvation of Transmembrane Proteins by Isotropic Membrane Mimetics: A Molecular Dynamics Study. *J. Phys. Chem. B* **2007**, *111*, 11285−11296.
(68) Stern, H. A.; Feller, S. E. Calculation of the Dielectric Permittivity Profile for a Nonuniform System: Application to a Lipid Bilayer Simulation. *J. Chem. Phys.* **2003**, *118*, 3401−3412.
(69) Nymeyer, H.; Zhou, H.-X. A Method To Determine Dielectric Constants in Nonhomogeneous Systems: Application to Biological Membranes. *Biophys. J.* **2008**, *94*, 1185−1193.
(70) Lousa, D.; Baptista, A. M.; Soares, C. M. A Molecular Perspective on Nonaqueous Biocatalysis: Contributions from Simulation Studies. *Phys. Chem. Chem. Phys.* **2013**, *15*, 13723−13736.